Journal of Catalysis 258 (2008) 256–264

Contents lists available at ScienceDirect

Journal of Catalysis

www.elsevier.com/locate/jcat

# Spectroscopic evidence for the adsorption of propene on gold nanoparticles during the hydro-epoxidation of propene

T.A. Nijhuis [a,*], E. Sacaliuc [b], A.M. Beale [b], A.M.J. van der Eerden [b], J.C. Schouten [a], B.M. Weckhuysen [b]

[a] Eindhoven University of Technology, Schuit Institute of Catalysis, Department of Chemical Engineering and Chemistry, Laboratory for Chemical Reactor Engineering, PO Box 513, 5600 MB Eindhoven, The Netherlands

[b] Utrecht University, Department of Chemistry, Inorganic Chemistry and Catalysis group, Sorbonnelaan 16, 3584 CA Utrecht, The Netherlands

ARTICLE INFO

*Article history:*
Received 30 May 2008
Revised 16 June 2008
Accepted 16 June 2008
Available online 15 July 2008

*Keywords:*
Gold
Propene
Epoxidation
XANES
In situ
Adsorption
Oxidation
Spectroscopy
Catalysis

ABSTRACT

The adsorption of propene on supported gold nanoparticles has been experimentally identified as a reaction step in the hydro-epoxidation of propene. This new finding was made possible by applying a detailed analysis of in situ measured XANES spectra. For this purpose, gold-on-silica catalysts were investigated since this support is more inert and propene is not converted. Propene adsorption was investigated by using the hydrogen oxidation as probe reaction. It was shown that co-feeding of propene dramatically decreased the hydrogen oxidation rate. Since it has been reported in the literature that the hydrogen oxidation occurs exclusively over gold nanoparticles, this inhibition by propene can be attributed to adsorption of propene on the gold nanoparticles. Delta-mu analysis of the in situ XANES spectra confirmed the adsorption of propene on the gold and the mode of adsorption was determined to be $\pi$-bonding. Comparative experiments with ethene and propane confirmed this $\pi$-bonded adsorption, since ethene similarly inhibited the hydrogen oxidation, while propane had only a minor effect. The direct observation of the adsorption of propene on gold nanoparticles corroborates our recent findings, in which we have shown that gold nanoparticles were activating propene to reactively adsorb on titania producing a bidentate propoxy species.



## 1. Introduction

Catalysts consisting of gold nanoparticles on titanium containing supports offer a highly attractive alternative possibility in the research to develop a new process to directly produce propene oxide [1–3]. These gold–titania catalysts epoxidize propene using a mixture of hydrogen and oxygen (Scheme 1). The current processes are complex and either have economic and/or operational disadvantages or environmental problems [4]. The hydroperoxide processes produce a co-product in a fixed stoichiometric amount, which makes the process less flexible. The chlorohydrin process produces chlorinated side products and a large salty waste stream. A new hydrogen peroxide combination process, under construction by Dow and BASF, first produces diluted hydrogen peroxide out of hydrogen and oxygen, which is fed directly as the epoxidizing agent into an epoxidation reactor, using Enichem TS-1 technology [5,6]. Although this process is clean and produces propene oxide as the only product, it is quite complex, utilizing three different reactors. In comparison, gold–titania catalysts produce propene oxide out of propene, hydrogen, and oxygen directly in a single reactor at mild conditions.

The gold–titania epoxidation catalysts, however, still have a few important issues which need to be addressed. First of all the conversion levels (typically <2%), the hydrogen efficiency (<30%), and finally the stability of the more active catalysts are usually low (the best system developed by Haruta et al. [7] produces propene oxide at a propene conversion of 10%, but loses about 40% of its activity in 4 h). A mechanistic understanding of this catalyst system can be of great help in the development of better catalysts, which do not suffer from these disadvantages.

The common view in the literature, is that the gold–titania catalysts are bifunctional: gold nanoparticles produce a peroxide species, which is subsequently transferred to titanium sites, which use the peroxide to epoxidize propene [2,8–10]. Indeed, in the literature it has been demonstrated that gold nanoparticles can produce hydrogen peroxide [10–13] and that titanium based catalysts are highly effective in epoxidizing propene using hydrogen peroxide [14]. Recently, Haruta et al. indeed detected the presence of peroxo species on these catalysts using in situ UV–vis spectroscopy [12]. A complete mechanistic picture, of this system, however, is not yet available.

$$H_2C{=}CH{-}CH_3 + H_2 + O_2 \xrightarrow{\text{Au–Ti catalyst}} H_2C\underset{\diagdown\,O\,\diagup}{-}CH{-}CH_3 + H_2O$$

**Scheme 1.** Hydro-epoxidation of propene over gold–titania catalysts.

* Corresponding author. Fax: +31 40 2446653.
*E-mail address:* t.a.nijhuis@tue.nl (T.A. Nijhuis).

0021-9517/$ – see front matter 
doi:10.1016/j.jcat.2008.06.020

In the literature, gold is generally thought to only play a role in the formation of the peroxide species [2,12,15]. Nijhuis et al. [16,17], however, published work based on infrared spectroscopy, which showed that gold has an additional role, namely, activating propene to adsorb on titania to produce a bidentate propoxy species. How this activation occurs, however, is not clear, and furthermore, if this bidentate propoxy species is indeed a reaction intermediate or rather a spectator, is also unclear. In the work of Mul et al. [18], the bidentate propoxy species is assumed to be the main species responsible for the catalyst deactivation. Although it is not clear if this bidentate propoxy species is either an intermediate or deactivating, both roles are of importance for the catalytic activity. The manner in which gold plays a role into the activation of propene to form the bidentate propoxy species can be either by propene which is adsorbing on the gold nanoparticles, or gold influencing the behavior of neighboring titanium sites.

From the literature, it is not clear if propene adsorbs on gold under the reaction conditions used for the epoxidation. In the work of Campbell et al. [19] on the adsorption of propene on gold nanoparticles supported on titania, propene adsorption is observed at temperatures up to 300 K, which is in agreement with the report of Davis and Goodman [20], whom observed propene adsorption at gold (111) and (100) surfaces up to 350 K. It is important to note that Campbell et al. [19] observed that propene primarily adsorbs on the perimeter of the gold nanoparticles, also interacting with the titania support. Davis and Goodman [20] made a distinction in the adsorption of propene on clean and oxygen covered gold surfaces. On clean gold surfaces propene already desorbed at 200 K, while in the presence of oxygen, the desorption was delayed up to 350 K. In this latter case, part of the 'propene' desorbed in the form of oxidation products. Friend et al. [21] studied the adsorption of propene on gold surfaces covered with atomic oxygen (created on the surface by ozone decomposition) and observed oxidized hydrocarbon species on the surface up to 500 K. In this study, however, the reactive atomic oxygen species towards propene, create stronger adsorbing species, similar to what Davis and Goodman reported. It is not known if during the hydro-epoxidation of propene, oxidized propene species will be formed on gold as well.

In this study, the hydrogen oxidation over gold on silica catalysts is used as probe reaction to obtain a better understanding into the gold–titania epoxidation system. Gold on silica catalysts were chosen in order to be able to investigate the interaction of hydrocarbons with the gold nanoparticles, without them being converted into propene oxide. A low reaction temperature of 353 K was used since it has been previously shown that such catalysts are only active for propene conversion at higher temperatures [17]. Catalytic experiments are performed and combined with in situ XANES measurements. The effect of feeding propene, as well as ethene and propane for comparison, on the catalytic activity is investigated as well as the in situ XANES spectra of the gold is investigated under reaction conditions in the presence and absence of these same hydrocarbons. Both will provide us with essential information if hydrocarbon (propene) adsorption on the gold nanoparticles is occurring and if it can play a role within the propene epoxidation reaction mechanism.

## 2. Experimental

### 2.1. Catalyst preparation

Catalysts were prepared using two types of silica, Degussa OX50 (50 $m^2/g$) and Davisil 645 (Grace Davison, 295 $m^2/g$). A catalyst was also prepared on P25 titania (Degussa, 45 $m^2/g$). Gold was deposited on the supports by means of a deposition precipitation method using ammonia [2].[1] 10 gram of support was dispersed in 100 ml of demineralized water with a magnetic stirrer. Using 2.5% ammonia the pH was raised to 9.5. The target loading in gold was 1 wt%, for which 172 mg of hydrogen tetrachloroaurate(III) solution ($HAuCl_4$, Aldrich—30 wt% solution) was diluted in 40 ml of demineralized water and added gradually over a 15 min period to the support slurry, while keeping the pH between 9.4 and 9.6 by periodically adding ammonia. After addition of all the gold, the solution was stirred for 1 more hour after which it was filtered and washed 3 times with 200 ml of demineralized water. The yellow catalyst was dried overnight in air at 353 K and then calcined. Calcination was carried out by heating to 393 K (5 K/min heating) for 2 h followed by 4 h at 673 K (5 K/min heating and cooling). The thus obtained catalysts had an intense dark color (brown-red for the Davisil and salmon pink/red for OX50).

### 2.2. Catalyst characterization

Scanning electron microscopy (SEM) and transmission electron microscopy (TEM) micrographs were taken of the catalysts to determine the gold particle size and distribution on the catalysts, both before and after use in catalytic experiments. X-ray fluorescence (XRF) analysis was used to determine the gold loading on the catalysts and the presence of contaminants affecting the activity (e.g., chloride).

### 2.3. Catalyst activity testing

A flow reactor was used to determine the catalytic performance of the different catalysts. The experiments were carried out with typically 0.30 g of catalyst and a gas flow of 50 Nml/min (GHSV 10,000 $h^{-1}$). A flow was used containing 5 vol% of hydrogen and 5 vol% of oxygen. Hydrogen oxidation experiments were performed with lower hydrogen and oxygen concentrations than is typically used for the hydro-epoxidation of propene to avoid operating too close to the explosion limits, which for hydrogen are lower compared to when no propene is present. Optionally ethene, propene, or propane was added in an amount of 5 vol%. The pressure in the reactor was 1100 mbar(a).

The analysis of the gas leaving the reactor was carried out using an Interscience Compact GC (gas chromatography) system, equipped with a Molsieve 5A and a Porabond Q column, each with a thermal conductivity detector (TCD). Gas samples were analyzed every 3 min. To make sure the catalyst was in a well defined state prior to the experiments, the catalysts were heated for 60 min at 573 K (10 K/min) in a 50 ml/min gas stream consisting of 10% of oxygen in helium. In prior work [16,17,22], it was determined that this treatment could restore the catalyst activity, even if it was deactivated during epoxidation experiments. The experiments performed with only the silica support material did not show any catalytic activity for either the propene epoxidation or the hydrogen oxidation. The catalytic tests were performed in a fully automated set-up over a period of typically 5–10 days during which multiple reaction conditions were applied, including repeat conditions to verify for catalyst deactivation.

[1] When gold catalysts are prepared using a deposition precipitation method with ammonia, it is possible that explosive, fulminating gold can form. Considering the small quantities of gold and the low loadings on the catalysts, the risks involved with the preparations in this paper are minor. However, an incident was reported in literature for this system (Fisher, Gold Bull. 36 (2003) 155) and caution is therefore advisable. Readers should therefore be aware of both the advantages (ease of making stable catalysts without chloride or sodium present) and disadvantages of this preparation method.

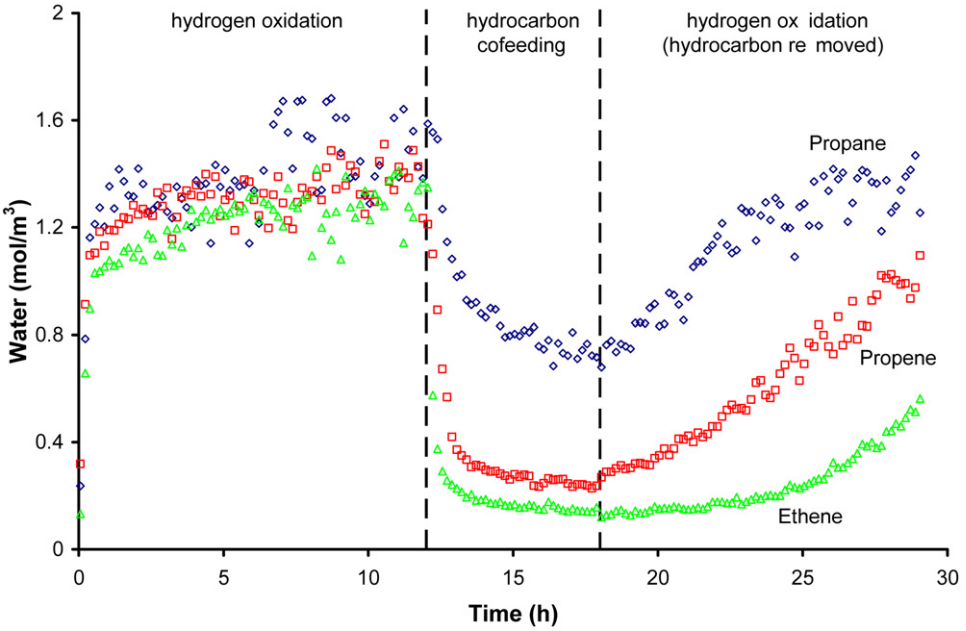


**Fig. 1.** Water formation rate (as water concentration in gas phase) in hydrogen oxidation over 1 wt% $Au/SiO_2$ (Davisil 645) catalyst at 353 K (GHSV = 16000 $h^{-1}$). From 12 to 18 h into the experiment a hydrocarbon is co-fed in the gas phase (propane, propene, or ethene) ($P = 1100$ mbar, 5% $H_2$, $O_2$, hydrocarbon in helium).

### 2.4. In situ XAFS analysis

XAFS measurements were performed on the working catalyst to evaluate if there were any changes in the gold particles during reaction. These measurements were performed on the Au $L_3$-edge (11.9187 keV) and were carried out on station BM26A at the ESRF (Grenoble, France). The measurements were performed in fluorescence mode using a multi-element Ge detector for the OX50 supported catalysts and in transmission mode using gas-filled ion-chambers including a monitor in order to correct for any variation in energy, for the Davisil supported catalysts. The measurements with the OX50 catalyst were performed in fluorescence mode, since the X-ray signal through the sample was too low to be reliably measured.

In the experiments a 200 mg sample was loosely pressed to form a self-supporting wafer/bed mounted in a specialized cell for recording in situ XAFS data. The XAFS spectra (out to 15 Å) were then recorded in normal scanning mode (ca. 40 min/spectrum) over a 48-h period under conditions comparable to those used for the catalytic activity tests (i.e. reaction temperature 353 K, gas composition 6 vol% hydrogen, 6 vol% oxygen and optionally 6 vol% hydrocarbon, remainder helium). XAFS data were processed using an in-house developed Matlab code. As with standard XAFS processing software the data was first converted into energy vs. absorption coefficient. The pre-edge was subtracted and the signal normalized to the post-edge background extrapolated to the edge position.

## 3. Results

### 3.1. Catalyst characterization

XRF analysis showed that the amount of chlorine present on the catalysts was below the detection limit of the system (<6 ppm). The gold loading of the catalysts was very close to the target loading of 1 wt% for the prepared catalysts (between 0.9 and 1 wt%). Table 1 gives the particle sizes for the prepared catalysts after calcination and after use in catalytic experiments (>150 h). It can be seen that the gold particle size is similar for both silicas and that during the catalytic experiments there is no significant change in the gold particle sizes. The EXAFS spectra recorded of the catalysts during the reaction did not change, indicating that the state of the bulk of the gold atoms remained the same. The Fourier transforms of the EXAFS spectra contained only contributions ascribable to Au–Au interactions (indicating only metallic gold being present) with a typical first shell coordination number of 10. The gold particle size, which could be estimated from the gold coordination in EXAFS, was found to be in agreement with the TEM results (typically 30% smaller).

**Table 1**
Overview of the sizes of gold nanoparticles and related errors (95% confidence limits) for the catalyst materials under study

| Catalyst | State | Average size (nm) | Error (std. dev.) | Particles counted |
|---|---|---|---|---|
| $Au/SiO_2$ (OX50) | Fresh | 4.0 | 0.2 (1.8) | 233 |
| | Spent | 3.7 | 0.2 (1.5) | 238 |
| $Au/SiO_2$ (Davisil) | Fresh | 3.5 | 0.3 (1.5) | 86 |
| $Au/TiO_2$ (P25) | Fresh | 3.9 | 0.1 (1.1) | 236 |
| | Spent | 4.2 | 0.2 (1.2) | 127 |

### 3.2. Catalytic testing

Fig. 1 shows the activity of the catalyst for the hydrogen oxidation. It can be seen that in the first part of the experiment after an initial activation the catalytic activity remains constant. The time it takes for the catalyst to reach about 80% of its final activity is about 30 min, which is considerably longer than the experimentally determined response time of the system to changes in the gas feed (less than 2 min). The hydrogen oxidation activity for the catalysts prepared supported on the two different types of silica (OX50 and Davisil 645) was identical.

Once propene is co-fed to the catalyst, the hydrogen oxidation rate drops dramatically by a factor of 3. Propene is not converted as far as it could be determined by GC analysis of the gases leaving the reactor. Once propene is removed from the gas feed, the catalytic activity of the hydrogen oxidation recovers slowly.

Comparable experiments were also performed for the hydrogen oxidation in which either ethene or propane was co-fed. Neither of

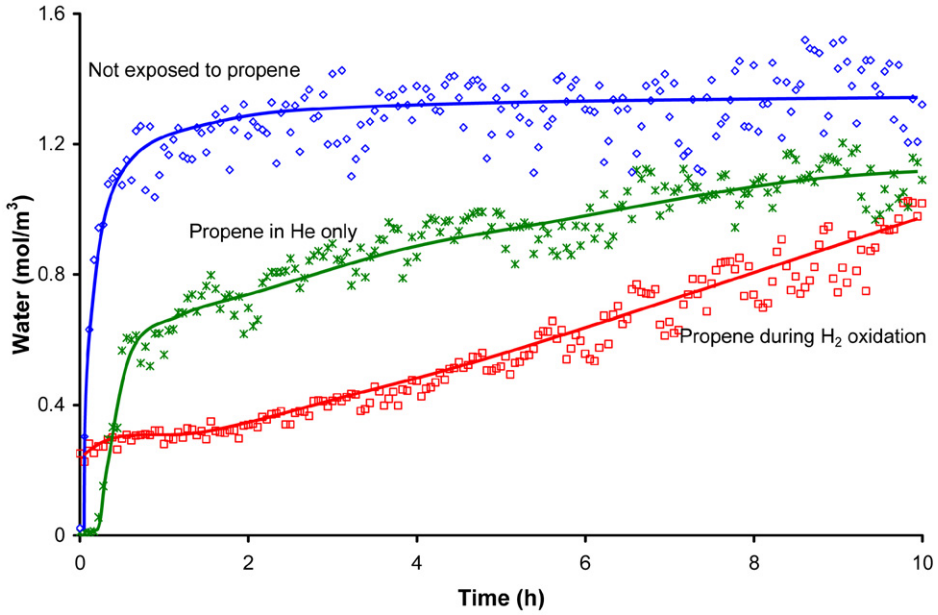


**Fig. 2.** Water formation rate (as water concentration in the gas phase) in hydrogen oxidation over 1 wt% $Au/SiO_2$ (Davisil 645) catalyst at 353 K (GHSV = 16000 $h^{-1}$). An experiment is shown in which a fresh catalyst is used, and experiment in which a fresh catalyst is exposed to propene (5% in He at 353 K) for 6 h prior to the hydrogen oxidation, and one in which, before the experiment shown, propene has been fed to the catalyst during the hydrogen oxidation for 6 h ($P = 1100$ mbar, 5% $H_2$, $O_2$, hydrocarbon in helium).

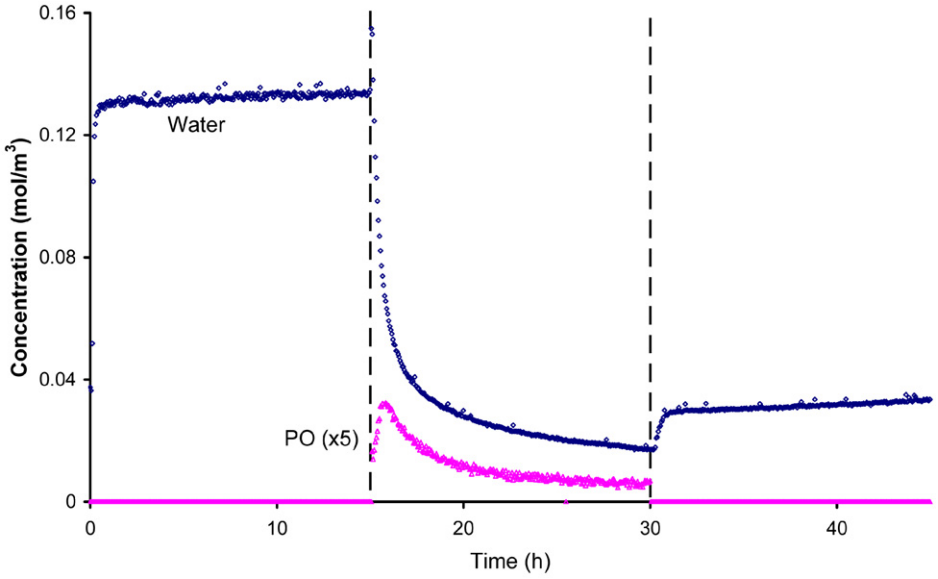


**Fig. 3.** Water and propene oxide formation rate (as concentration in gas phase) in hydrogen oxidation over 1 wt% $Au/TiO_2$ (P25) catalyst at 323 K (GHSV = 16000 $h^{-1}$). In the first and final part of the experiment only the hydrogen oxidation is performed (no propene present). From 15 to 30 h into the experiment propene is co-fed in the gas phase and propene oxide is produced ($P = 1100$ mbar, 5% $H_2$, $O_2$, hydrocarbon in helium).

the hydrocarbons were converted. For ethene, it was observed that the hydrogen oxidation dropped similarly as for propene. The activity recovery after ethene removal was considerably slower than for propene. For propane, the decrease in the catalytic conversion that could be observed was significantly less, approximately 25%. Furthermore, the catalytic activity is recovered about 4 h after the removal of the propane. Duplicate experiments were performed, which showed that for each of the hydrocarbons the extent of hydrogen oxidation inhibition was reproducible quantitatively with an identical rate of activity recovery after the hydrocarbon was removed.

In Fig. 2 an experiment is shown in which propene is fed over a gold/silica catalyst, prior to exposing the catalyst to the hydrogen oxidation. This experiment makes it possible to determine if the propene adsorption on gold is affected by the presence of activating oxygen/peroxide species, which are present when hydrogen and oxygen are present. It can be seen that compared to a catalyst that has not been exposed to propene (or another hydrocarbon), the activity is lower. However, the catalyst that was exposed to propene during the hydrogen oxidation, has a catalytic activity that is even lower.

Fig. 3 shows the performance of a $Au/TiO_2$ catalyst as is commonly used in propene hydro-epoxidation studies in an experiment in which it is first exposed to a hydrogen oxidation, then to the epoxidation, and thereafter again to the hydrogen oxidation. It can be seen that for this catalyst propene is also strongly inhibiting the hydrogen oxidation. Furthermore, after removal of the propene from the gas feed, the activity remains very low.

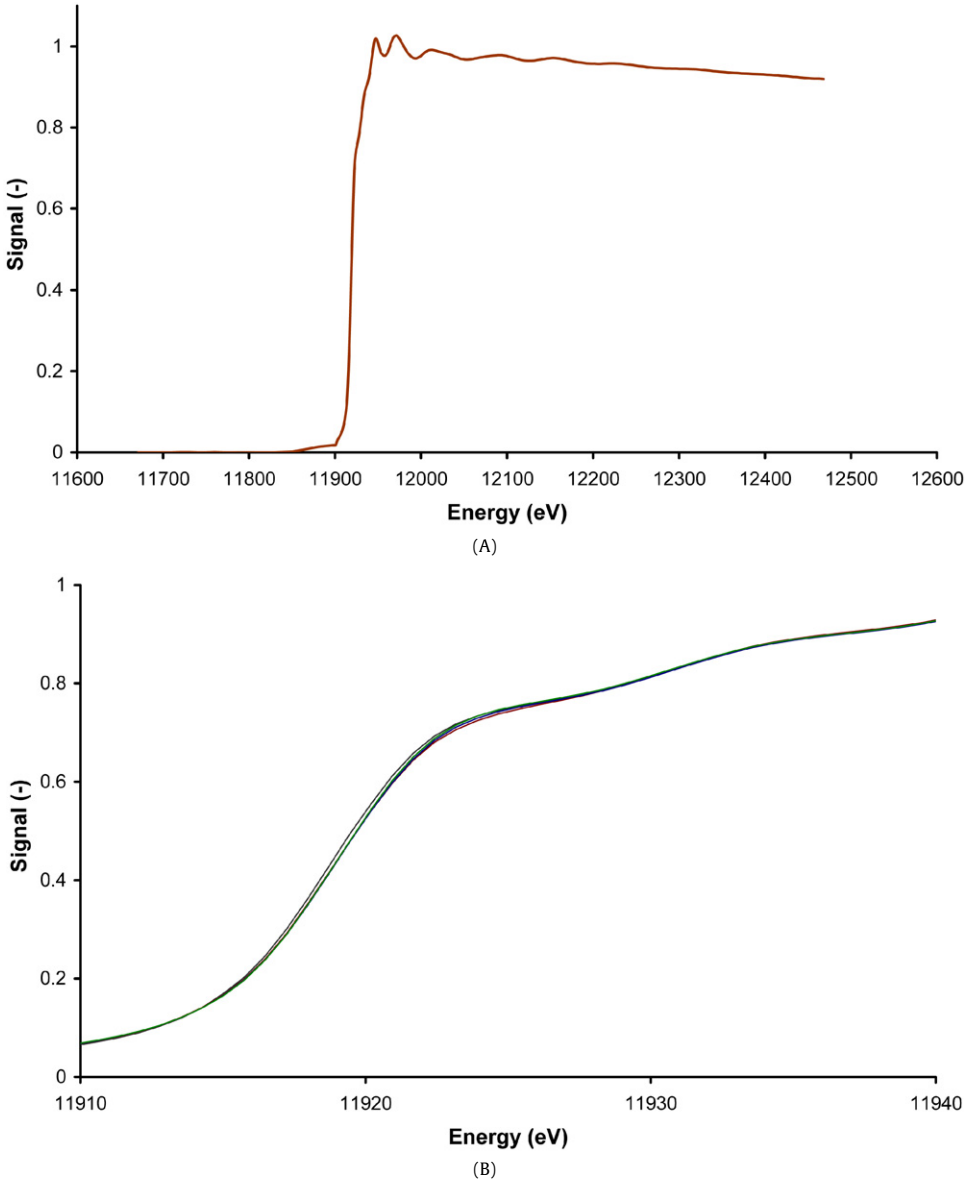


**Fig. 4.** (A) XAFS spectrum of gold/$SiO_2$ (Davisil 645) catalysts in helium over the entire recorded range from 11650 to 12500 eV. (B) Magnification of the XANES region (11850–1200 eV) of the XAFS spectra in helium, during the hydrogen oxidation, during propene co-feeding in hydrogen oxidation, and after propene removal in hydrogen oxidation (curves overlapping).

### 3.3. XAFS analysis

In Fig. 4 the in situ XAFS spectra recorded during an experimental series of a hydrogen oxidation over Au/$SiO_2$ (Davisil 645) with intermediate propene co-feeding are shown. It can be seen that in the 'raw' XAFS spectra no significant changes can be observed in the spectra during the entire experiment. This indicates that even though during the reaction the catalytic activity of the gold particles is changing significantly, neither the oxidation state (metallic gold vs. cationic) nor the size of the particles is changing significantly.

In Fig. 5, the delta-mu XANES spectra are shown of the catalyst during this activation phase. In a delta-mu XANES spectrum [23], the changes in the XANES region of the spectrum are made more pronounced by subtracting a reference spectrum of the same catalyst, usually recorded on the same sample in the same experimental run but under different conditions. The delta-mu spectra shown in Fig. 5 are the spectra recorded with the starting spectrum (the catalyst in helium) as a reference subtracted. It can be seen that the delta-mu XANES spectrum slowly develops a feature at 11,920.2 eV. The intensity of this developing feature increases together with the increasing catalytic activity as shown in Fig. 1. An explanation of this feature can be given by a small shift of the edge position of 0.15 eV to a higher energy. In another experimental series measured earlier at the same beamline but recorded on the gold on OX50 silica catalyst in Fluorescence mode (not shown) this shift was determined to be 0.2 eV. This shift is very small considering the energy resolution of the beamline of 0.8 eV. However, the shift is occurring over a wide range of data points and can therefore still be determined accurately numerically. Furthermore the feature only starts to develop from the moment the hydrogen–oxygen feed is initiated and the development is gradual, which further supports the validity of the observation. The simultaneous measurement of a gold reference foil, placed in the beam after the sample and before a third detector (monitor) eliminates the possibility that such changes are caused by either a 'drift' in the energy calibration of the beamline.

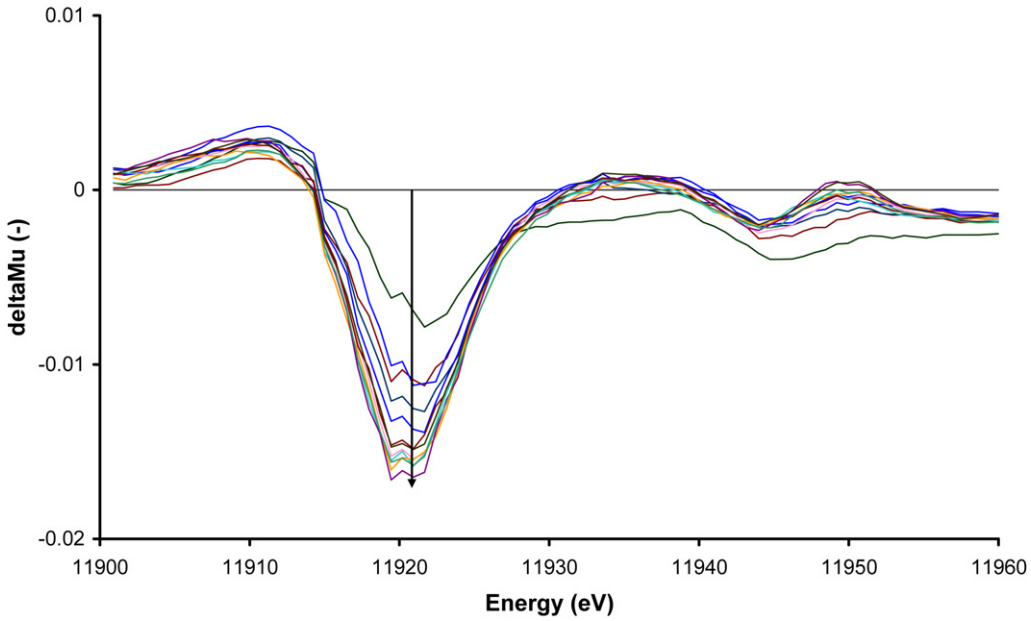


**Fig. 5.** Development of features in delta-mu XANES spectrum of the Au $L_3$-edge of a $Au/SiO_2$ (Davisil 645) catalyst during the activation in the hydrogen oxidation reaction. The first spectrum (horizontal line) He spectrum is used as a starting position. Spectra thereafter are collected after 50 min intervals for each spectrum.

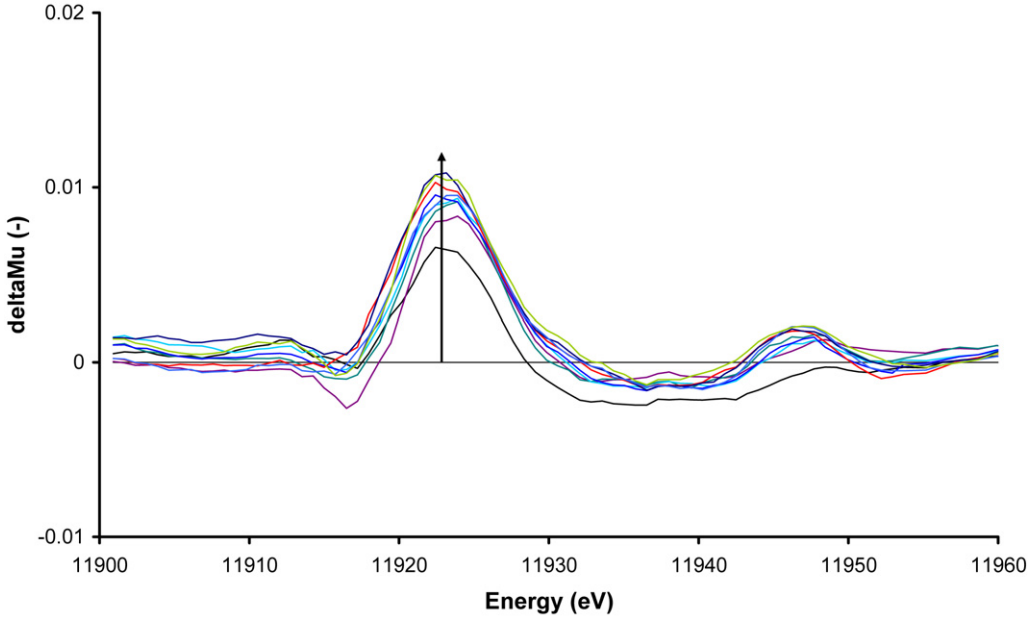


**Fig. 6.** Development of features in delta-mu XANES spectra of the Au $L_3$-edge of a $Au/SiO_2$ (Davisil 645) catalyst during the co-feeding of propene during the hydrogen oxidation reaction. The first spectrum (horizontal line) is the steady state spectrum during the hydrogen oxidation, which is used as a starting position (reference). Spectra thereafter are collected after 50 min intervals for each spectrum.

In Fig. 6 the delta-mu spectra are shown during the hydrogen oxidation experiment when propene is co-fed. In this figure, the XANES spectra of the catalysts in its steady state condition during the hydrogen oxidation, are used as the reference. It can be seen that in the presence of propene, a feature is appearing at 11922.4 eV, attributable to the appearance of a whiteline in the XANES spectrum. When propene is removed from the gas-phase, this feature disappears after about 1 h. The location of this feature is over 2 eV above the edge position and again cannot be explained by any shift in the position of the adsorption edge.

In Fig. 7 the delta-mu spectra are shown for the developed feature after exposure of the gold catalyst to ethene, propene, and propane. It can be seen that the features for propene and ethene are very similar. For propane, the feature is much less intense and the position is slightly shifted.

## 4. Discussion

### 4.1. Catalytic data

In the catalytic experiments, it can be seen that the hydrocarbons containing a double bond, strongly inhibit the hydrogen oxidation over gold. Propane co-feeding only has a minor effect on the reaction rate. The most likely conclusion from these observations is that the hydrocarbons adsorb on the gold nanoparticles via an interaction with their double bond. The fact that no other reaction products other than water are observed is a clear indication

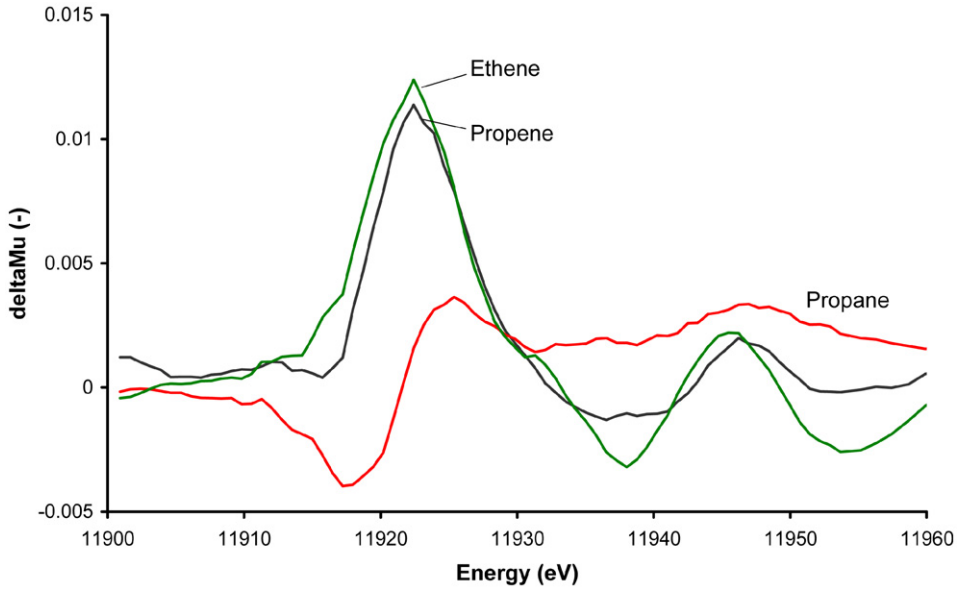


**Fig. 7.** Delta-mu XANES spectra of the Au $L_3$-edge of a $Au/SiO_2$ (Davisil 645) catalyst during the co-feeding of propene, propane, and ethene during the hydrogen oxidation reaction. The steady state spectrum during the hydrogen oxidation prior to the hydrocarbon feeding was used as a starting position (reference).

that the hydrocarbon adsorption occurs via a reversible (physical) absorption on the gold particles. Given the extent of the inhibition on the hydrogen oxidation rate, and the time it takes until the catalytic activity is restored from the moment the hydrocarbon co-feeding is stopped, this implies that the hydrocarbon absorption is strong.

If one compares the behavior of a gold–titania catalyst exposed to a similar reaction cycle (Fig. 3), it can be seen that the inhibiting effect of propene on the hydrogen oxidation is very similar. However, during the propene co-feeding (when the epoxidation also occurs) the catalyst deactivates significantly; the propene oxide formation decreases and the water formation rate decreases even further. This type of deactivation is commonly observed for gold–titania epoxidation catalysts [2,22]. Upon removal of the propene for this catalyst, the hydrogen oxidation rate undergoes only a minor recovery after which the activity remains at a much lower level, indicating that in this case a deactivating species remains on the catalyst. The catalyst activity can be fully restored by a simple treatment at 573 K in 10% oxygen in helium for 30 min. This proves that the deactivation is not caused by an irreversible change to the catalyst itself (e.g., sintering of the gold particles), but rather by the formation of a hydrocarbon related deactivation product. In the literature, this species is usually attributed to either propene oxide oligomers [2,8] or carbonates formed out of consecutive oxidation of propene oxide [16,22].

Although the inhibiting effect by ethene and propene is reversible, the fact that the hydrogen oxidation activity is not restored to its original level even after over 10 h of continued hydrogen oxidation after the hydrocarbon is removed, indicates that the inhibition occurs by more than a simple physical absorption. Attempts to determine the presence of the adsorbed species by infrared spectroscopy so far were unsuccessful. After removal of the hydrocarbon, no adsorbed species could be detected on the catalyst. In the presence of the hydrocarbon, the intensity of the signal from the gaseous hydrocarbon was too strong to allow the observation of adsorbate species.

In Fig. 2, it is seen that the inhibiting effect of exposing the catalyst to propene only on the hydrogen oxidation activity is less strong than in the case when propene is co-fed during the hydrogen oxidation. A possible explanation for this might be that during the hydrogen oxidation reactive peroxo species are present on the gold nanoparticles, which would convert part of the adsorbed propene to even stronger adsorbed partially oxidized species. However, we could not prove this assumption by spectroscopic (infrared or XAFS) data, which would imply that the amount of such a species on the catalyst would be very low.

### 4.2. Delta-mu XANES analysis

The delta-mu XANES analysis of XAFS data has been principally exploited by Ramaker et al. [23] in order to interpret subtle changes in the XANES spectrum, which can be the result of the adsorption of species on small metal particles. Recently Van Bokhoven et al. [24] performed a delta-mu XANES analysis on gold on titania catalysts for the CO oxidation reaction. In this work they reported the appearance of a positive feature in the delta-mu XANES spectrum at 11920 eV when their catalyst was exposed to oxygen only, which was interpreted in terms of the formation of an activated Au-O complex on the reducible support. In our work, we observe a negative peak in the delta-mu XANES at the same position (Fig. 5). The appearance of this negative peak during the 'activation phase' of the hydrogen oxidation, however, needs an alternative explanation. In the work of Guzman and Gates [25,26] the activity of gold catalysts for CO oxidation is linked to the presence of cationic gold species. A slight shift of the gold edge to a higher energy, our explanation for the negative peak in the delta-mu XANES at 11920 eV, is in agreement with the presence of an initially small amount of oxidized (positively charged) gold species being reduced. Costello et al. [27] reported on the shifting gold edge upon reduction of a gold catalyst. Guzman and Gates [25,26] found a direct link between the catalytic activity for the CO oxidation and the presence of cationic gold in the nanoparticles, which indicates how a slight shift in the overall oxidation state can have a large effect on the catalytic performance.

Upon exposure of the catalyst during hydrogen oxidation to ethene or propene, a positive feature is appearing in the delta-mu XANES spectrum at 11922.4 eV. This feature is different from the negative one at 11920 eV that appeared during the 'activation phase' in the hydrogen oxidation and not just its reversal. In the work by van Bokhoven on the CO oxidation [24] an identical feature appeared at 11922.5 eV upon exposing the catalyst to CO. In this work this feature was explained by the back-bonding of the

gold d-band to the $2\pi^*$ molecular orbitals of CO reducing the density of d-states, making the $2p_{3/2}$–5d dipole transition allowed. In later work by van Bokhoven et al. [28], they observed a feature which is identical to our observation in Fig. 6 upon exposing gold and platinum catalysts to ethene. According to theoretical references they obtained using calculations with the FEFF8 program, they were able to attribute the spectrum to pi-bonded ethene on gold or platinum.

In our work, we observe this same delta-mu XANES spectrum when we expose our gold on silica catalyst to ethene or propene. This makes it possible to conclude that also under the reaction conditions used for the hydrogen oxidation over gold, both ethene and propene are bonding to the gold particles by means of $2\pi^*$–d-backbonding, which explains why they both can have a strong inhibiting effect on the hydrogen oxidation. Since propane does not have a double bond, this molecule cannot pi-bond to gold, which explains why its inhibiting effect is significantly less and also why in the delta-mu XANES spectrum no strong features are visible. Since in the hydrogen oxidation over gold on silica, we used identical conditions as they are used for the propene epoxidation over gold–titania catalysts, it can be assumed that also during the propene hydro-epoxidation propene will adsorb on the gold nanoparticles.

In Fig. 2 we noticed that the inhibiting effect of propene on the hydrogen oxidation is stronger when propene is co-fed during the hydrogen oxidation than when propene is fed to the catalyst in absence of hydrogen and oxygen. We assume therefore, that the inhibition might be partly by adsorbed propene and partly by a stronger adsorbing species produced by a partial conversion of the propene on the gold nanoparticles in the presence of hydrogen and oxygen. This assumption is in line with the fact that in the delta-mu XANES spectrum we see the feature disappearing at 11922.4 eV (attributed to propene adsorbed by pi-bonding) in just over 1 h time. In Fig. 2, we can also see that when we just expose the catalyst to propene, the catalyst recovers 50% of its final activity in less than 1 h time. We were not able to find evidence of a more strongly adsorbing 'second' inhibiting species formed in the presence of propene, hydrogen, and oxygen in the delta-mu XANES spectra, which would indicate that such a species would be present on the surface of the gold nanoparticles only in very small amounts. Since we did not observe any changes in either the EXAFS or the XANES of the spectra before and 1 h after the exposure of the catalyst to propene during the hydrogen oxidation, we think it is unlikely the state of the gold nanoparticles itself has changed because of this exposure to propene.

### *4.3. Implications for relevance for propene epoxidation reaction mechanism*

In our earlier work [16,17], we reported on an infrared spectroscopic study on the (reactive) adsorption of propene on gold–titania catalysts. We observed that in the presence of gold nanoparticles, propene could adsorb on titania producing a bidentate propoxy species, which is the same species formed upon adsorption of propene oxide on titania. This bidentate propoxy species was only formed in the presence of gold nanoparticles; no measurable adsorption of propene occurred in the absence of these nanoparticles. Oxygen and or hydrogen were not required to produce this species. Two explanations were offered for the formation of this species. The first option was that propene would adsorb on gold and in an activated adsorbed form be transferred to titania for a reactive adsorption producing the bidentate propoxy species. The second option was that the gold nanoparticles would influence the state of the neighboring titanium atoms, making them more reactive towards propene to form a bidentate propoxy species. In this work, we observed the adsorption of propene on gold nanoparticles on an inert support. Therefore, our current proposal for the formation of bidentate propoxy species is that this occurs via an adsorption of propene on gold, followed by a spill over to titania. Therefore, we propose a second function of the gold nanoparticles, in addition to the commonly described peroxide formation over the gold nanoparticles out of hydrogen and oxygen [13,29,30]. Since in this work we did not study the epoxidation itself, it cannot yet be determined whether the bidentate propoxy species formed in this manner is a reaction intermediate [16,17] or the species responsible for catalyst deactivation [18].

## 5. Conclusions

Both propene and ethene were found to strongly inhibit the hydrogen oxidation rate over gold nanoparticle catalysts. By analysis using delta-mu XANES, it was determined that both propene and ethene are $\pi$-bonding to the gold particles. Propane adsorption was not observable in the XANES analysis, which is in agreement with the minor inhibiting effect that propane has on the hydrogen oxidation rate. The inhibition of (adsorbed) propene on the hydrogen oxidation is stronger when propene is exposed to the catalyst in the presence of both hydrogen and oxygen, in comparison to the inhibiting effect propene has when it is fed to the catalyst prior to the hydrogen oxidation. This indicates that in the presence of hydrogen and oxygen a small fraction of the propene might be converted to an even stronger adsorbing species, although this remains speculative, since we could not confirm the presence of this species using direct spectroscopic measurements.

The adsorption of propene on gold nanoparticles under reaction conditions typical for the propene hydro-epoxidation can be a key step in the epoxidation reaction mechanism. This adsorption supports the observation we reported earlier [16,17] that gold nanoparticles on titania can make propene reactively adsorb on titania to produce a bidentate propoxy species. The adsorption of propene on the gold nanoparticles, significantly reduces the direct water formation over gold catalysts, which is an undesirable competitive reaction during the hydro-epoxidation of propene.

## Acknowledgments

STW/NWO is kindly acknowledged for the VIDI grant supporting the research of T.A.N. NWO is kindly acknowledged for providing beam-time at the DUBBLE XAFS station (BM-26A) at the ESRF facility in Grenoble. C. van de Spek is thanked for performing the TEM analysis.

## References

[1] A.S.K. Hashmi, G.J. Hutchings, Angew. Chem. Int. Ed. 45 (2006) 7896–7936.
[2] T.A. Nijhuis, B.J. Huizinga, M. Makkee, J.A. Moulijn, Ind. Eng. Chem. Res. 38 (1999) 884–891.
[3] A.K. Sinha, S. Seelan, S. Tsubota, M. Haruta, Top. Catal. 29 (2004) 95–102.
[4] T.A. Nijhuis, M. Makkee, J.A. Moulijn, B.M. Weckhuysen, Ind. Eng. Chem. Res. 45 (2006) 3447–3459.
[5] A.H. Tullo, P.L. Short, Chem. Eng. News 84 (2006) 22–23.
[6] A. Tullo, Chem. Eng. News 82 (2004) 15.
[7] A.K. Sinha, S. Seelan, S. Tsubota, M. Haruta, Angew. Chem. Int. Ed. 43 (2004) 1546–1548.
[8] E.E. Stangland, K.B. Stavens, R.P. Andres, W.N. Delgass, J. Catal. 191 (2000) 332–347.
[9] C. Sivadinarayana, T.V. Choudhary, L.L. Daemen, J. Eckert, D.W. Goodman, J. Am. Chem. Soc. 126 (2004) 38–39.
[10] J. Edwards, P. Landon, A.F. Carley, G.J. Hutchings, J. Mater. Res. 22 (2007) 831–837.
[11] P. Landon, P.J. Collier, A.J. Papworth, C.J. Kiely, G.J. Hutchings, Chem. Commun. (2002) 2058–2059.
[12] B. Chowdhury, J.J. Bravo-Suarez, N. Mimura, J.Q. Lu, K.K. Bando, S. Tsubota, M. Haruta, J. Phys. Chem. B 110 (2006) 22995–22999.
[13] T. Ishihara, Y. Ohura, S. Yoshida, Y. Hata, H. Nishiguchi, Y. Takita, Appl. Catal. A 291 (2005) 215.

[14] M.G. Clerici, G. Bellussi, U. Romano, J. Catal. 129 (1991) 159–167.
[15] J.Q. Lu, X.M. Zhang, J.J. Bravo-Suarez, S. Tsubota, J. Gaudet, S.T. Oyama, Catal. Today 123 (2007) 189–197.
[16] T.A. Nijhuis, T. Visser, B.M. Weckhuysen, Angew. Chem. Int. Ed. 44 (2005) 1115–1118.
[17] T.A. Nijhuis, T. Visser, B.M. Weckhuysen, J. Phys. Chem. B 109 (2005) 19309–19319.
[18] G. Mul, A. Zwijnenburg, B. van der Linden, M. Makkee, J.A. Moulijn, J. Catal. 201 (2001) 128–137.
[19] H.M. Ajo, V.A. Bondzie, C.T. Campbell, Catal. Lett. 78 (2002) 359–368.
[20] K.A. Davis, D.W. Goodman, J. Phys. Chem. B 104 (2000) 8557–8562.
[21] X.Y. Deng, B.K. Min, X.Y. Liu, C.M. Friend, J. Phys. Chem. B 110 (2006) 15982–15987.
[22] T.A. Nijhuis, B.M. Weckhuysen, Catal. Today 117 (2006) 84–89.
[23] A. Teliska, W.E. O'Grady, D.E. Ramaker, J. Phys. Chem. B 109 (2005) 8076–8084.
[24] N. Weiher, A.M. Beesley, N. Tsapatsaris, L. Delannoy, C. Louis, J.A. van Bokhoven, S.L.M. Schroeder, J. Am. Chem. Soc. 129 (2007) 2240–2241.
[25] J. Guzman, B.C. Gates, J. Am. Chem. Soc. 126 (2004) 2672–2673.
[26] J. Guzman, B.C. Gates, J. Phys. Chem. B 106 (2002) 7659–7665.
[27] C.K. Costello, J. Guzman, J.H. Yang, Y.M. Wang, M.C. Kung, B.C. Gates, H.H. Kung, J. Phys. Chem. B 108 (2004) 12529–12536.
[28] E. Bus, D.E. Ramaker, J.A. van Bokhoven, J. Am. Chem. Soc. 129 (2007) 8094–8102.
[29] G.J. Hutchings, Chem. Commun. (2008) 1148–1164.
[30] A.M. Joshi, W.N. Delgass, K.T. Thomson, J. Phys. Chem. B 109 (2005) 22392–22406.